

Design of the VenSpec-U instrument: A double UV imaging spectrometer to analyze sulfured gases in the Venus' atmosphere

B. Lustrement^a, S. Bertran^b, N. Rouanet^a, A. Díaz Damián^a, R. Hassen-Khodja^a, C. Montaron^a, S. Ruocco^a, A. Vontrat^a, F. Vivat^a, L. Baggio^a, G. Guignan^a, E. Simonnet^b, L. Conan^{a,e}, C. Gabier^a, A. Langlois^c, R. Mathon^c, N. Nguyen Tuong^d, W. Recart^b, T. Buey^d, S. Vinatier^d, J. Lasue^c, L. Lara^h, E. Marcq^a, S. Robert^f, and J. Helbert^g

^aLATMOS/IPSL, UVSQ Université Paris-Saclay, Sorbonne Université, CNRS, Guyancourt, France

^bHensoldt Space Consulting, 11 boulevard d'Alembert, Guyancourt, 78280, France

^cIRAP, OMP, CNRS, Université de Toulouse III. 9, Av. du Colonel Roche, 31028 Toulouse Cedex 4

^dLESIA, CNRS, Sorbonne Université, Université Paris Cité. 5 place Jules Janssen, 92195 Meudon Cedex, France

^eCentre National d'Études Spatiales (CNES). 18 avenue Edouard Belin 31401 Toulouse Cedex 9, France

^fRoyal Belgian Institute for Space Aeronomy (IASB-BIRA), Avenue Circulaire 3, 1180 Brussels, Belgium

^gDeutsche Zentrum für Luft und Raumfahrt, Rutherfordstraße 2, 12489 Berlin, Germany

^hInstituto de Astrofísica de Andalucía, Granada, Spain

ABSTRACT

VenSpec-U is one of the three channels of the VenSpec suite onboard the ESA's mission Envision to Venus, whose launch is foreseen in 2031. It is a UV spectrometer operating in the 190-380 nm range aiming at analyzing the sulfured gases in the high atmosphere of Venus by absorption spectroscopy and investigating the unknown "UV absorber", thus contributing to answer one of the key questions the Envision mission will address: "How

Send correspondence to E. Marcq

E-mail: emmanuel.marcq@latmos.ipsl.fr, Telephone: (+33)1 80 28 52 83

Infrared Remote Sensing and Instrumentation XXXII, edited by Marija Strojnik, Jörn Helbert, Proc. of SPIE Vol. 13144, 131440K · © 2024 SPIE 0277-786X · doi: 10.1117/12.3028252

has Venus' climate become so hostile". VenSpec-U, developed under LATMOS (Guyancourt, France) PI-ship, is part of the spectrometer suite named "VenSpec" led by DLR (Berlin, Germany). This manuscript provides an overview of the current instrument design, at the time of the end of phase B1/early phase B2.

Keywords: Instrumentation, UV spectrometer, Planetary Atmospheres, Venus

1. INTRODUCTION

1.1 The Envision Mission

The EnVision mission lies at the heart of the ESA Cosmic Vision programme whose objectives are to identify the conditions for planet formation and the emergence of life, and to understand how the Solar System works. In this context, EnVision is dedicated to the study of Venus. Its three main scientific themes are:

Activity How geologically active is Venus today?

History How have the surface and interior of Venus evolved?

Climate How has Venus' climate become so hostile?

The Envision mission¹ has been selected as the fifth "M-class" mission by the European Space Agency (ESA) in June 2021 and went through adoption in early 2024. The launch is scheduled for 2031.

Envision is composed of a spacecraft accommodating four payloads to study the Venus system in an holistic approach (Fig. 1): a synthetic aperture radar *VenSAR*, a subsurface radar sounder *SRS*, a radio-science experiment *RSE* and the UV/IR spectrometers suite *VenSpec*.

After launch, the spacecraft will start a cruise phase of 2 years followed by an aerobraking phase of 2 years before orbit insertion in 2035. It will be placed on a low quasi-polar Venus orbit with inclination between 87 and 89°, with altitudes varying from 220 to 540 km and orbital period of about 92 min.

1.2 The VenSpec suite

The VenSpec suite,² led by DLR (Deutsches Zentrum für Luft- und Raumfahrt), will address some of the *Activity* and most of the *Climate* topics by performing spectrometry measurements from the Venus surface to cloud top layer. The VenSpec suite comprises the infrared mapper VenSpec-M, Infrared "High Resolution" Spectrometer VenSpec-H and the UV Imaging Spectrometer VenSpec-U (Table 1). In addition, the electrical interface (power and data) between the S/C and the channels is ensured by the VenSpec Central Command Unit (CCU, Fig.2).

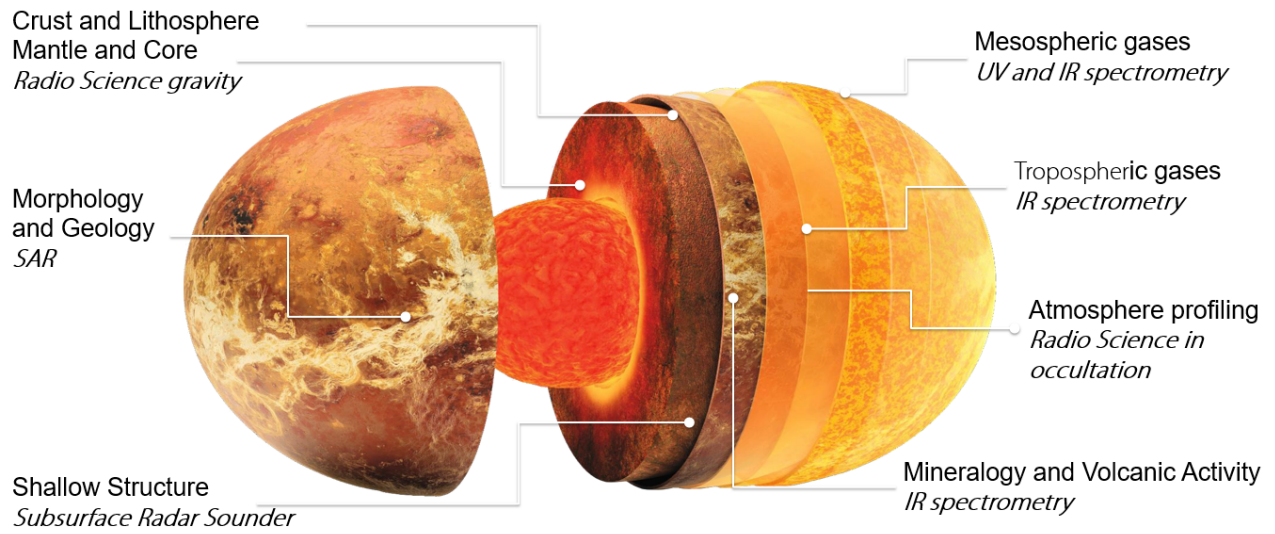


Figure 1. Holistic approach to address the Venus system, from EnVision's Red Book¹

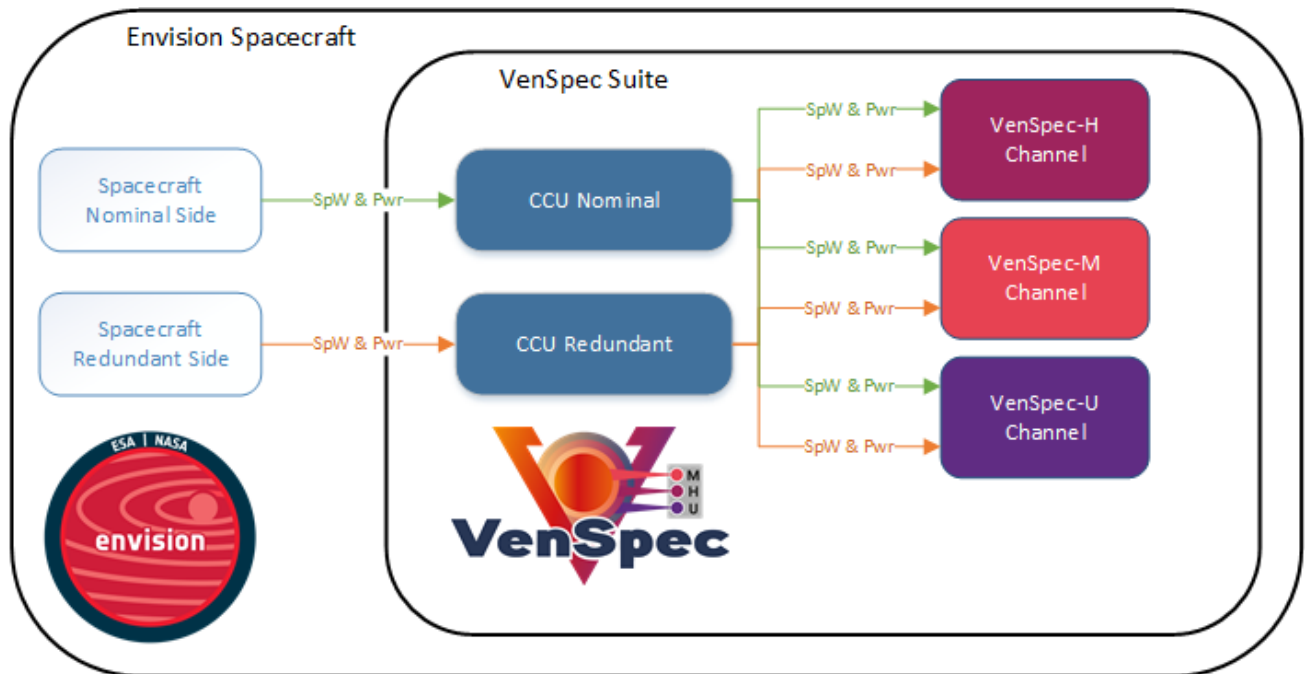


Figure 2. The VenSpec Suite and its Central Command Unit (CCU). SpW: Spacewire bus, Pwr: Power bus

Table 1. The VenSpec suite instruments

Suite element	Scientific targets and objectives	Instrument lead / Institute	Instrument type
Venspec-CCU	Electrical interfacing of the Suite to the S/C	Jörn Helbert	Central Control Unit ³
VenSpec-M	Mineralogy and volcanic activity	DLR, Berlin, Germany	IR Emissivity mapper ⁴
VenSpec-H	Trace gases monitoring	Séverine Robert BIRA-IASB, Brussels, Belgium	High Spectral Resolution IR spectrometer ⁵
VenSpec-U	Mesospheric gases (SO, SO:SO ₂) and unknown UV absorber monitoring	Emmanuel Marcq LATMOS, Guyancourt, France	Dual channel UV spectral imager ⁶

1.3 VenSpec-U science objectives and requirements

The VenSpec-U instrument will search for atmospheric effects of geological activity, in order to determine how much outgassing is occurring, and how the atmospheric chemistry is coupled with surface/subsurface geochemistry and weathering cycles, as expressed in the EnVision Red Book:¹

- Study how mesospheric gas variations are linked to volcanism, in order to identify the causes of variability in the mesospheric sulphured gases (SO, SO₂).
- Study how cloud and particulate variability is linked to volcanism, in order to detect plumes of volcanic ash or sulphate clouds caused by volcanism, and to understand any link between the Venus sulphuric acid clouds and volcanism.

The following science objectives have already been addressed in the context of past UV observations in Ref. 6. Here we are restating them in the more general context of the *EnVision* mission and *VenSpec* suite investigations.

1.3.1 SO₂ monitoring

The strong variability of SO₂ above the clouds of Venus has been known since the early 1980s through the measurements performed with the UV spectrometer OUVS on board *Pioneer Venus Orbiter*⁷ and in IR by *Venera*

15.⁸ After a decade with almost no new observations, cloud top SO₂ monitoring resumed with the UV spectrometer SPICAV on board *Venus Express*.^{9–11} IR spectroscopic observations from Earth based telescopes have also been used to acquire planet-wide "snapshots" of SO₂ abundance near cloud top.^{12,13} All these observations reached similar conclusions:

- SO₂ long and short scale temporal variability at lower latitudes is remarkably high, spanning about three orders of magnitude;
- conversely, high-latitude SO₂ (beyond $\pm 50^\circ$) remains at low levels, about one order of magnitude above the detection threshold;
- most low latitude variability occurs in localized (≤ 1000 km) and transient (lasting a few Earth days) SO₂ "plumes". The changing rate in the plumes occurrence is responsible for the long-term variability of low-latitude SO₂;
- evidence for correlation with surface topography is ambiguous, since most data were acquired from a polar orbit, thus mixing longitudinal and long-term variability due to the slow orbital precession.

This variability pattern is consistent with a short lifetime of SO₂ above the clouds, ranging from a few hours to a few Earth days. This hints at fast photochemical reactions acting as an immediate sink for SO₂ (see Sec. 1.3.2). Supplying cloud top with new SO₂ molecules originating from the lower atmosphere, where SO₂ is steadily available in much larger quantities,¹⁴ is therefore dependent on deep vertical mixing through the poorly known cloud layers. This vertical mixing is expected to vary strongly with time and location, depending on the changing static stability profile,^{15–17} and could be sensitive to external forcings such as thermal buoyancy anomalies caused by volcanic activity.¹⁸

On the other hand, fluctuations on vertical mixing may also occur as spontaneous atmospheric oscillations caused by closed feedback loops such as the one shown in Fig. 3. A better characterization of SO₂ spatial and temporal variability is required to assess the actual mechanisms at work behind these SO₂ variations.

1.3.2 SO:SO₂ monitoring

As previously mentioned in Sec. 1.3.1, the immediate sink for SO₂ above the clouds of Venus starts with its photochemical dissociation by UV sunlight: $\text{SO}_2 + h\nu = \text{SO} + \text{O}$ (see e.g. Ref. 19). In order to better understand sulphur chemistry, measuring the relative abundance of SO:SO₂ is therefore of paramount importance. Unfortunately, SO absorption spectrum in the UV range overlaps the much more prominent SO₂ absorption band near

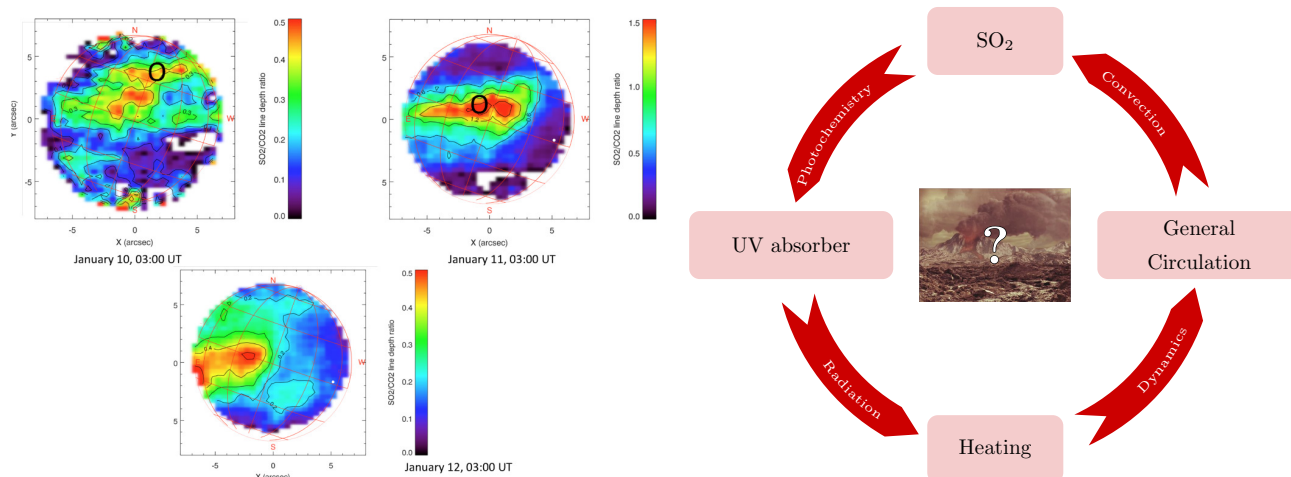


Figure 3. *Left:* SO₂ plumes as observed by TEXES/IRTF;¹² *Right:* putative closed feedback loop yielding spontaneous oscillations of these known to vary variable atmospheric variables.

220 nm, so that a high spectral resolution is needed in order to separate the individual absorption lines of these two species.

Such observations have been performed using the STIS UV spectrograph onboard the Hubble Space Telescope,²⁰ and found a column abundance ratio SO:SO₂ close to 1 : 10 in average, and varying between 1 : 4 and 1 : 25. These observations are too sparse, and their error bars too large (> 50%) to assess whether the SO:SO₂ is correlated with other observable parameters.

Besides their own scientific interest, colocated SO₂ and SO measurements would also help in reducing systematic uncertainties in SO₂ UV retrievals: due to their comparatively lower spectral resolution, most of the aforementioned studies in Sec. 1.3.1 assumed a constant SO:SO₂ ratio (usually 1 : 10) consistent with the average value found with STIS/HST. But these SO₂ retrievals are probably contaminated by the yet poorly constrained variability in SO:SO₂ ratio.

1.3.3 UV absorber monitoring

Venus' upper clouds are known to host a species (or several species) that displays a characteristic absorption in the blue and near UV range,²¹ peaking near 365 nm. The chemical nature of this species is still unknown, and although several candidates have been proposed^{22, 23} such as salts like FeCl₃ or linked to the sulphur cycle like OSSO, no consensus about its composition has been reached (as of 2024).

In any case, the UV markings near 365 nm are more long-lived than the sulphured gaseous species SO and SO₂, lasting longer than the cloud top superrotation period of 4 Earth days. They can therefore be used for *cloud tracking*, thus allowing for wind speed measurements at this altitude level (assuming microphysical processes such

as condensation and evaporation are comparatively slow). Besides large scale circulation measurements,^{24,25} the morphology of the UV absorber spatial contrasts have revealed the existence of sub-solar convection cells as well as various atmospheric waves that will be discussed in next Sec.1.3.4.

Another scientific interest of the UV absorber consists in studying its long term variations (on a decennial timescale): since most orbiters since the *Pioneer Venus* era have carried UV-sensitive instruments (e.g. VMC/Venus Express²⁶ and UVI/Akatsuki²⁷), and since this wavelength range can also be observed through Earth's atmosphere, long term monitoring of the Venus albedo at 365nm could be performed and revealed a decennial variability ranging up to 0.2 in absolute value.^{28,29} Determining the physical origin for these variations, and their possible link with other variable quantities such as SO₂ or zonal wind speed^{11,30} is therefore of paramount importance in order to understand Venus' climate.

1.3.4 Small spatial scale observations

As mentioned in section 1.3.3, numerous dynamical structures have been observed at cloud top level in the 365 nm-centered absorption band of the unknown UV absorber. First of all, convective-like structures were observed by the VMC instrument on board *Venus Express*³¹ near the subsolar point (close to the equator near 12 local solar time), typically extending 20 km across. Linear wave fronts were also observed with a typical wavelength ranging from 3 to 21 km, found preferentially above high surface elevations.³² This provided a first hint to an unsuspected coupling between topography and atmospheric circulation at cloud top level later seen in thermal infrared brightness³³ by LIR/*Akatsuki*. The fact that such small scale spatial contrasts are seen for the UV absorber raises the question of the existence of such contrasts for other observable parameters at cloud top level in the UV range, such as local column densities of SO₂ and SO above the clouds, as well as cloud top altitude.

Such observations would be also highly useful in constraining the free parameters in large eddy or mesoscale simulations coupling small scale dynamics with local processes such as photochemistry or microphysics. Such models are already being developed^{16,34} but have to rely on some assumptions (e.g. boundary conditions outside the modeled zone, set of considered chemical reactions, parametrization of microphysical processes) that are still poorly known as of 2024. New observations at these small spatial scales would therefore help in constraining these assumptions in return, providing precious knowledge about the interplay of small scale dynamics, chemistry and clouds.

1.3.5 Requirement flowdown

Figure 4 shows the derivation of science requirements to top level mission and measurement requirements:

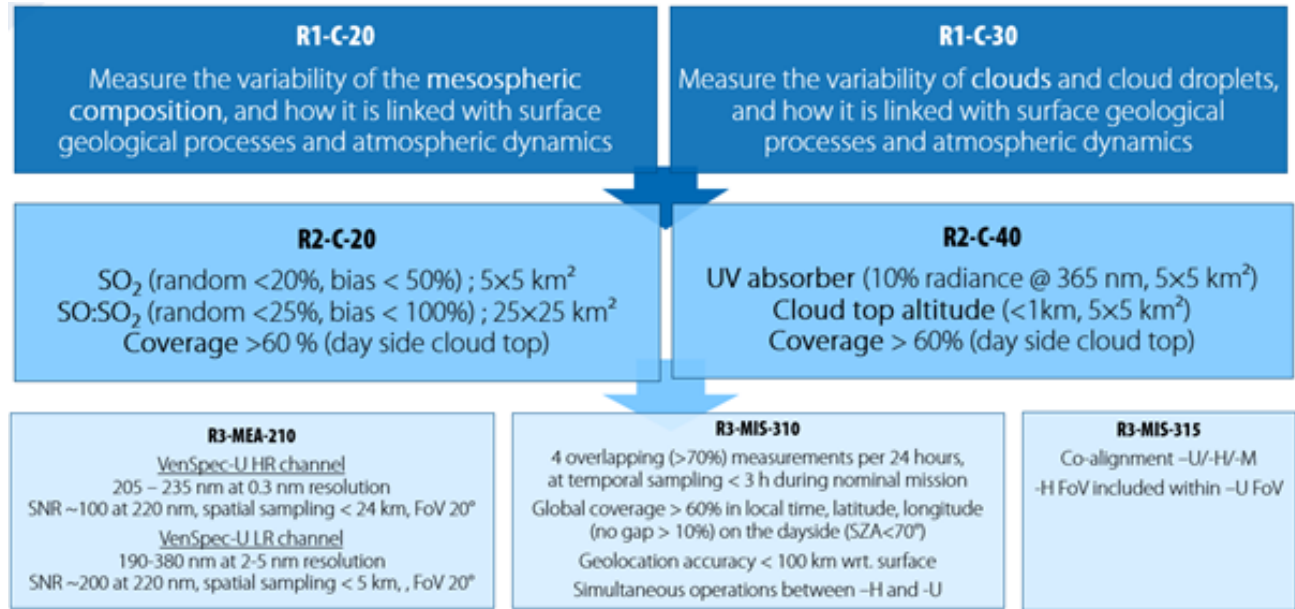


Figure 4. VenSpec-U science requirements flowdown chart, from [1]

A detailed justification of how science objectives (level 1 and level 2 requirements) are linked to instrumental or mission requirements (level 3) in terms of spectral range and resolution, Signal-to-Noise ratio can be found in [6], with recent updates including a first estimation of systematic bias allowance in the companion paper [35].

1.4 VenSpec-U measurement and operation concept

VenSpec-U science relies on the measurement of the Venus Radiance Factor β (Eq.1) defined as the ratio between the spectral radiance L measured by the instrument on day side and the estimated Sun irradiance F_{\odot} . At the time of the operational phase, the Sun spectral irradiance will be provided by a combination of third-party measurements and modelling to minimize measurement errors.

$$\beta(\lambda) = \frac{L(\lambda) \times \pi \text{sr}}{F_{\odot}(\lambda)} \quad (1)$$

The instrument being operated in a so-called "pushbroom" observation strategy (Fig.5), the narrow-slit axis of the instrument contains the spectral information, whereas the long-slit axis contains the spatial information along the 20° field of view ("across-track"). The remaining spatial direction ("along-track") is provided through orbital scrolling.

Measurements will be performed over four consecutive orbits (over fifteen orbits a day) such that the wide across-track FoV allows for an overlapping of 4/5th between two consecutive orbits, thus enabling discrimination

of variability patterns linked to surface (which should persist) and those linked to purely atmospheric phenomena (which should be carried away by the zonal superrotation out of the transverse 20° field of view).

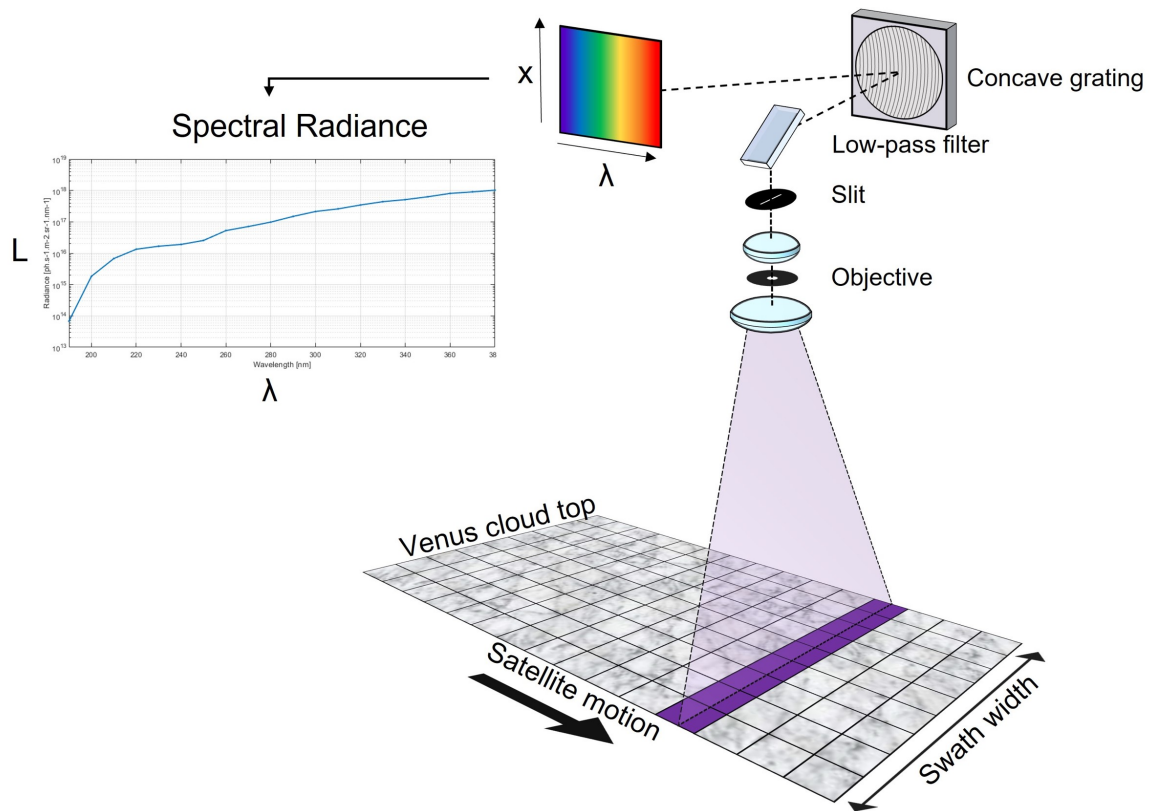


Figure 5. Pushbroom observation principle

2. INSTRUMENT TOP LEVEL REQUIREMENTS AND RESOURCES ALLOCATIONS SUMMARY

For reference, the top level performance requirements and allocations are presented in table 2 and 3.

3. INSTRUMENT DESIGN

3.1 Instrument concept and design drivers

VenSpec-U (figure 6) is a single unit whose compact "all-included" design is inherited from LATMOS-provided UV spectrometer PHEBUS onboard Bepi Colombo³⁶. The Electronic box (Ebox) supports the Optical box (Obox) thus limiting the overall mass and envelop at the expense of a greater complexity of the mechanical and thermal design. VenSpec-U is a "flat-mounted" unit conductively coupled to the spacecraft. It is accommodated inside a spacecraft cavity with baffles protruding out of the nadir panel thus benefiting of a quite stable thermal environment. The spacecraft provides two thermal interfaces (table 4).

Table 2. Top level instrument performance requirements

	Requirement	LR Channel	HR Channel
Spectral requirements	Spectral range	190 - 380 nm	205 - 235 nm
	Spectral resolution	2 nm (190 - 320 nm) 5 nm (320 - 380 nm)	0.3 nm
Spatial requirements	Swath FoV	20°	20°
	Spatial sampling on cloud top (70 km)	5 × 5 km ²	24 × 24 km ²
Radiometric and accuracy requirements	SNR	typ. 200 @ 220 nm	typ. 100 @ 220 nm
	Biases and systematic errors	Combination of measurement biases shall satisfy ESRA requirements ³⁵	
	Absolute radiometric accuracy	10% at 365 nm	-

Table 3. VenSpec-U System budget

Budget	Allocation	Comment
Power (Venus observation)	25.6 W	At VenSpec-U Interface
Data rate (Venus observation)	0.347 Mbps	At VenSpec-U Interface "Typical" observation mode
Data volume (Venus observation)	978 Mbit	At VenSpec-U Interface Per half orbit "Typical" Observation mode
Envelope	291 × 468 × 353 mm ³	
Mass	9.32 kg	

Achieving top level instrument requirements (Section 2) within provided allocation required a dual-channel concept (namely the "Low spectral Resolution" channel "LR" and the "High spectral Resolution" channel "HR") with a single shared CMOS detector (sections 3.2, 3.6.1) allowing for specific control and readout of the two detector areas based on a Rolling Shutter (RS) scheme. Both channels will be co-aligned and nominally operated simultaneously.

Each channel (Fig.7) consists of (1) an entrance baffle used to limit the stray-light coming from the Venus disk or any other bright source out of the field of view; (2) an objective composed of two lenses and a stop

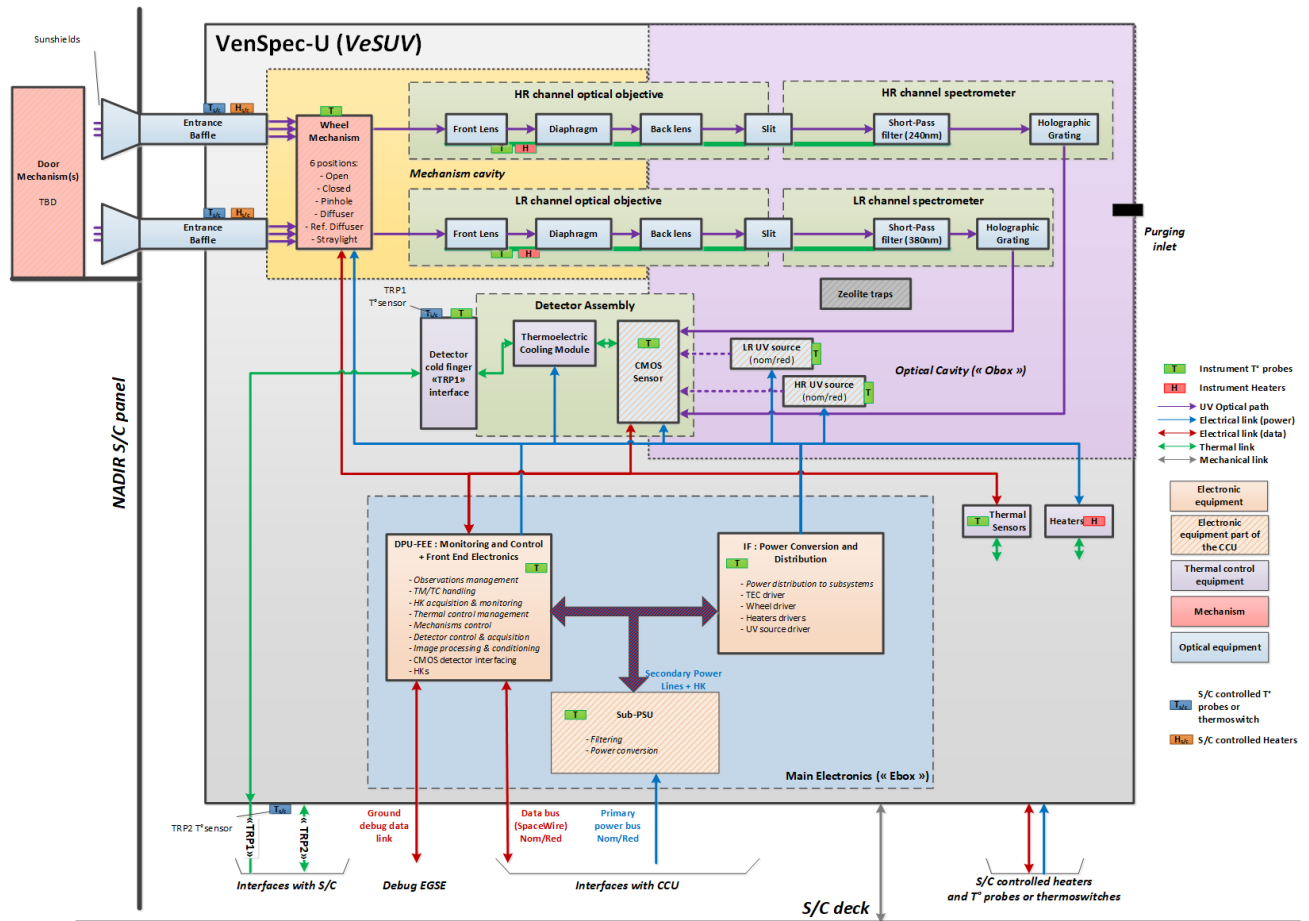


Figure 6. Block diagram
Table 4. TRPs definition and temperature ranges

Temperature Ref. Point	Purpose	Operational temp. range	Non-operational temp. range
TRP1	Cold detector interface	[-10°C; 0°C]	[-30°C; +50°C]
TRP2	Main thermal interface (instrument)	[0°C; +40°C]	[-30°C; +50°C]

diaphragm, the requested wide FoV is then provided by the entrance slit; (3) a spectrometer mainly composed of this slit and a spherical holographic grating in charge of dispersing the slit image onto the detector. The spectrometer also comprises a short-pass filter to attenuate light whose wavelength is above the higher limit of the spectral bands of interest (> 235 nm for the HR channel, > 380 nm for the LR channel) and a light trap used to avoid stray-light due to the zeroth-orders emerging from the grating. The dispersion planes of both channels

are offset by 12 mm such that the spectra are formed on the focal plane one above the other (fig.7).

Radiometric calibration of the instrument performed on the Sun during dedicated spacecraft slews is enabled thanks to the use of two sets of optical diffusers and one set of pinholes (section 3.2). These optical components are positioned in front of the objectives during calibration operations thanks to the wheel mechanism (section 3.6.2). This wheel mechanism is also used to open the optical apertures during Venus observations and to close for dark calibration or when not observing, thus preventing the optics from being contaminated.

A low dark current and stable behaviour of the detector are guaranteed by cooling and regulating its temperature down to -25°C . This is achieved thanks to the Peltier cooler (or Thermo-Electric Cooler, TEC) embedded in the CMOS detector package (section 3.6.1) which is coupled to the cold thermal interface provided by the S/C at TRP1.

Small UV sources using LED's (section 3.6.3) are accommodated in the Obox for each channel. They will provide homogeneous irradiance of the detector and will be used for functional testing and in-flight characterization of the sensor (Pixel Response Non Uniformity tracking, Photon Transfer Curve, ...).

VenSpec-U design is "cleanliness driven" (section 3.5): both particulate and molecular contamination have a strong impact on instrument performances, leading to optical chain efficiency reduction (particularly in the UV), increased stray-light, and flat-fielding issues, finally degrading measurement accuracy.

Anti-contamination heaters installed on the baffles prevent contaminants from depositing onto the baffles surface after launch, while the overall spacecraft outgasses materials. Decontamination heaters are installed on the objectives, enabling decontamination of lenses' and filters' surfaces if deemed necessary during the mission.

The control/command of the instrument relies on a set of three electronic boards located side-by-side in the Ebox (section 3.4).

3.2 Optical design

3.2.1 Objectives

The design philosophy of VenSpec-U objectives prioritizes a simple design while achieving the scientific requirements in terms of imaging quality across the observational spectral band and the FoV. This approach has resulted in a consolidated design composed of two lenses and an aperture stop between them (the real entrance pupil of the system being located roughly at the front surface of the rear lens). Both lenses are singlets crafted from UV grade fused silica and treated with an anti-reflection coating. The front lens (L1) is plano-convex with a spherical front surface; the rear lens (L2) is biconvex with an aspherical front surface and a spherical back surface. Both objectives are almost identical, their only differences are the aperture stop diameter and the back focus (adapted

to each channel). The objectives have an average focal length of 22.7 mm across the spectral band and the FoV of 20°; their average F-numbers are F/4.7 for LR and F/5.2 for HR. Optical design parameters are summarized in table 5.

3.2.2 Spectrometer

For each channel, the spectrometer section of the instrument is composed of the entrance slit located at the focal plane of its objective, a reflective short pass dielectric filter working at 45° incidence, a spherical aberration corrected holographic grating and a common CMOS image sensor (see sec. 3.6.1). LR and HR channels slits are both 8 mm high but different widths of 180 and 224 μm respectively. The bandpass of the filters is designed to attenuate wavelengths above 380 nm for LR and 260 nm for HR (5% max. reflection). The arm lengths of the spectrometers are approximately 200 mm for LR and 300 mm for HR. The gratings were designed to optimize the diffraction efficiency of the 1st diffraction order in the spectral band of each channel, this optimization was achieved by choosing the best coating (Aluminum for both) and groove profile. The gratings groove densities are 485 gr/mm for LR and 2142 gr/mm for HR. The useful spectrum produced by each channel on the detector focal plane spreads over an area of 20 mm along the spectral axis by 8 mm along the spatial axis.

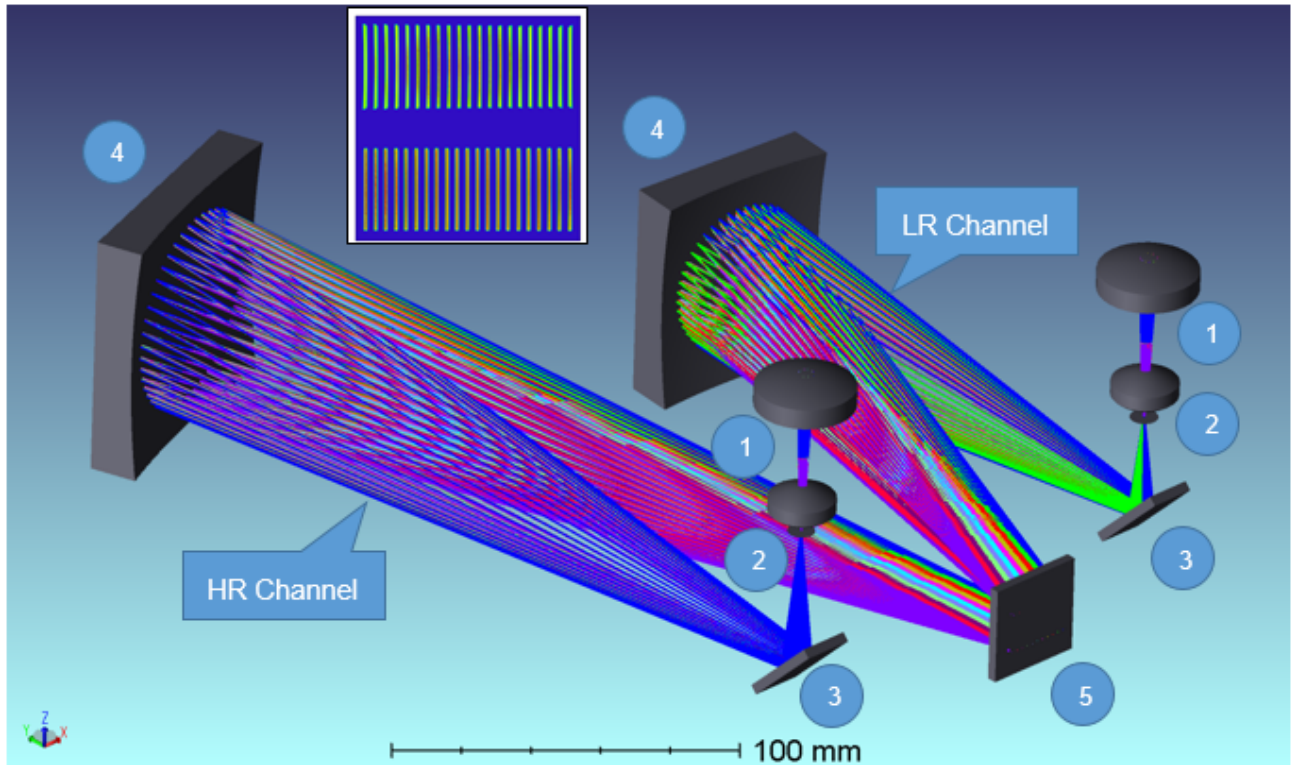


Figure 7. Optical layout overview, LR/HR channels and spectra relative positions on the detector (1: objectives / 2: Slits / 3: Filters / 4: Gratings / 5: Common detector)

Table 5. VenSpec-U Optical system parameters

Properties	Units	LR	HR	Comments
Spectral range	nm	190 – 380	205 – 235	
Spectral resolution	nm	2	0.3	FWHM
Entrance objective focal length	mm	22.7	22.7	
Entrance pupil diameter	mm	4.8	4.4	
Entrance objective F-Number		4.7	5.2	
Slit size	mm × μ m	8 × 180	8 × 224	
Field of view	°	20	20	Spatial axis
Spectrometer arm length	mm	200	300	
Grating groove density	gr/mm	485	2142	
Spectrum spread	mm × mm	20 × 8	20 × 8	Spectral × Spatial
Linear dispersion	mm/nm	0.105	0.667	

3.2.3 Solar calibration optics

To perform in-flight calibrations the instrument is pointed towards the Sun and either an optical diffuser or a pinhole will be placed in front of the entrance objectives with the wheel mechanism. The goal of the diffuser is to act as a lambertian secondary source inside the 20° FoV in order to generate a flat field of the spectrometer. The pinhole has a 100 μ m diameter for LR and 400 μ m for HR, it is used to perform absolute radiometric calibration; its role is to reduce the quantity of light received from the Sun to avoid saturating the detector. The solar calibration operations are described in section 5.2.

3.2.4 Straylight management

Early in the development, a stray-light analysis has been done to refine the design of the instrument. The current design, now showing good performances in terms of stray-light management (figures 8, 9), includes the following:

1. Multi-stages baffles accommodated in front of the optical apertures to reject out-of-field straylight;
2. High-absorption black coating (Acktar Magic BlackTM) where needed, black anodizing anywhere else;
3. Short-pass filters to reject out-of-band light;
4. Internal helical baffle to avoid channel cross-contamination;
5. Zeroth orders management with high-absorption surfaces;

6. Stringent requirements on optics to limit diffusion and ghosts;
7. Particulate and molecular contamination management.

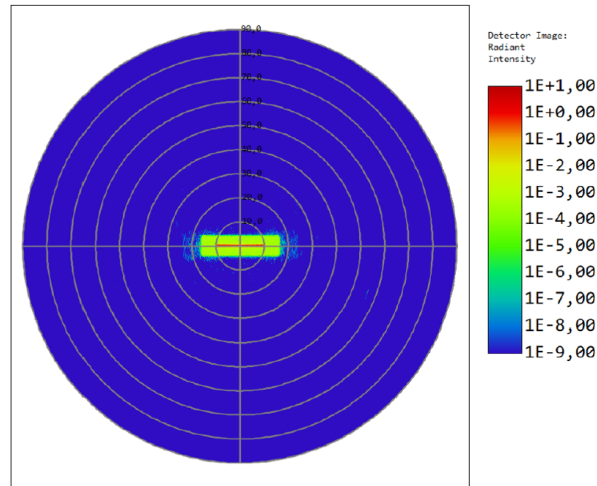


Figure 8. Map of the contribution of the different points of the observed scene to the total power through the slit (arbitrary units), logarithmic scale, at 190 nm

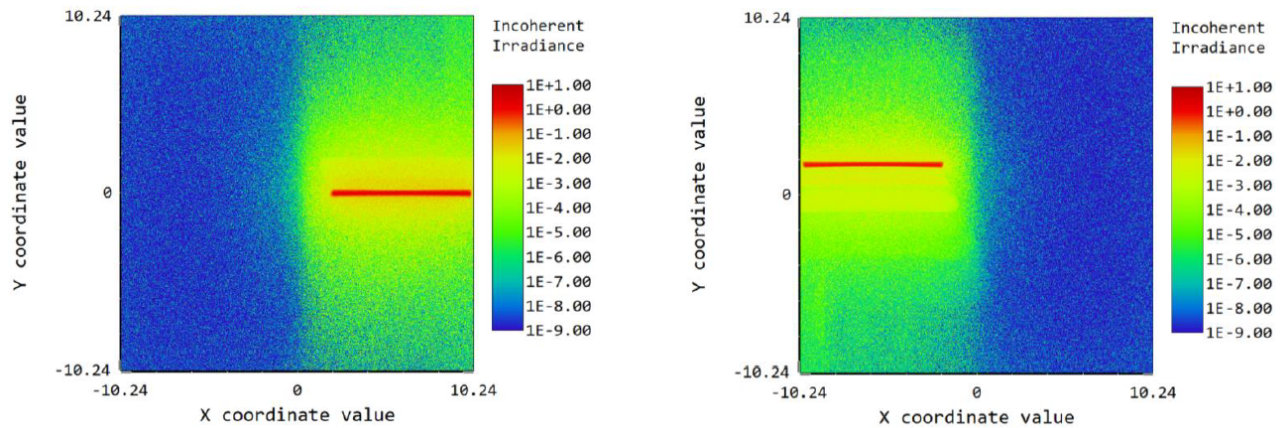


Figure 9. Examples of simulated Irradiance Maps on the detector (arbitrary units), logarithmic scale, all light paths, for the LR channel with signal at 270 nm (left) and HR channel with signal at 220 nm (right)

3.3 Mechanical and thermal design

The VenSpec-U is an "internally-mounted", single unit instrument composed of two major assemblies : the Ebox and the Obox, figure 10. The Ebox is made of aluminum and includes all the electronics boards, accommodated side-by-side within a same plane (figure 11). It is thermally coupled to the spacecraft at TRP2 (table 4), thus offering good thermal conduction to evacuate heat from the boards. The Obox sits on top of the Ebox. It has

an L-shape due to the optical design implying the use of reflection filters (figures 12, 13). The Obox optical bench is made of titanium to manage thermo-elastic deformation that would introduce misalignment between the optics while the temperature of the instrument spans in the operational range, thus degrading the instrument performances. Flexures are used between the Ebox and the Obox to allow them contracting/dilating freely without introducing extra deformations. At the time of writing this paper, a mechanical and a thermal analyses are in progress to validate this new design. The baffles, protruding out of the nadir deck of the spacecraft are thermally decoupled from the main structure of the instrument thanks to brackets made of titanium (figure 13), thus preventing high heat fluxes to warm-up the instrument excessively (Sun pointing, aerobraking). The detector package is also decoupled from the main structure and is coupled to a cold interface provided by the spacecraft (TRP1, table 4 and figures 10, 12).

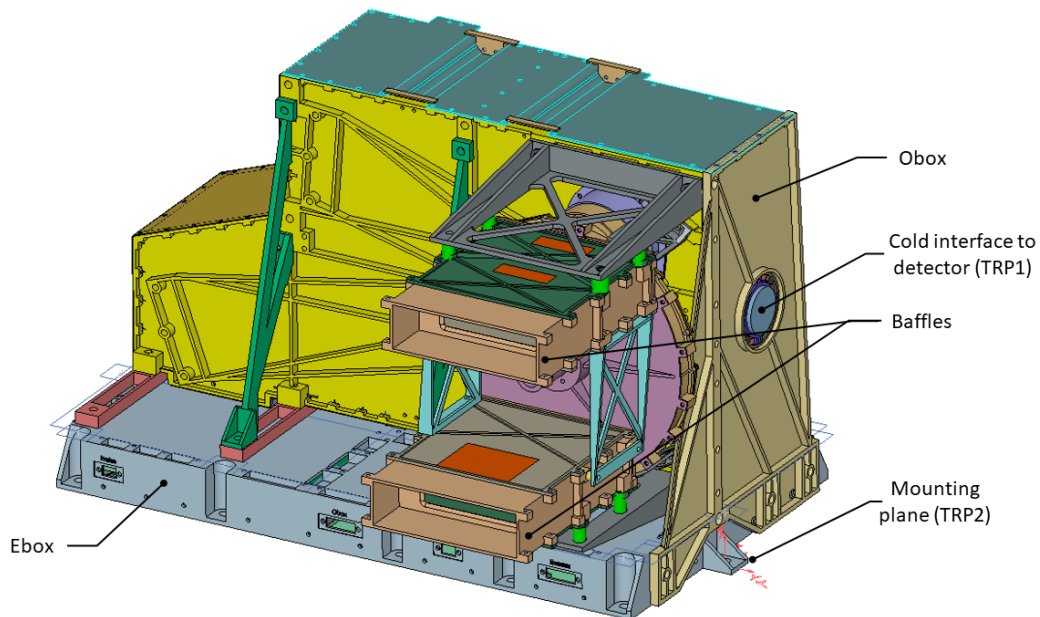


Figure 10. CAD view of the instrument

The detector is the reference and is hard mounted on the structure. Alignment of the objectives' elements is mostly guaranteed by design (lenses, slits). Alignment of the optical system is guaranteed by:

1. A custom interface to be manufactured for each objective assembly allowing co-alignment of the two channels;
2. The mounts of the filters providing two degrees of freedom (tilts);
3. the mounts of the gratings providing the four degrees of freedom.

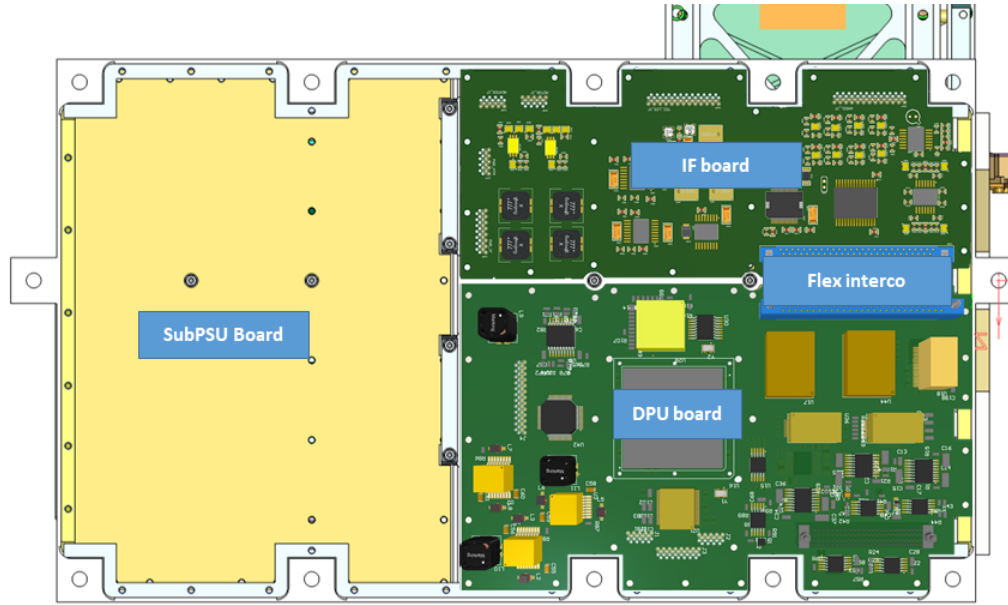


Figure 11. CAD view of the Ebox showing electronics boards accommodation

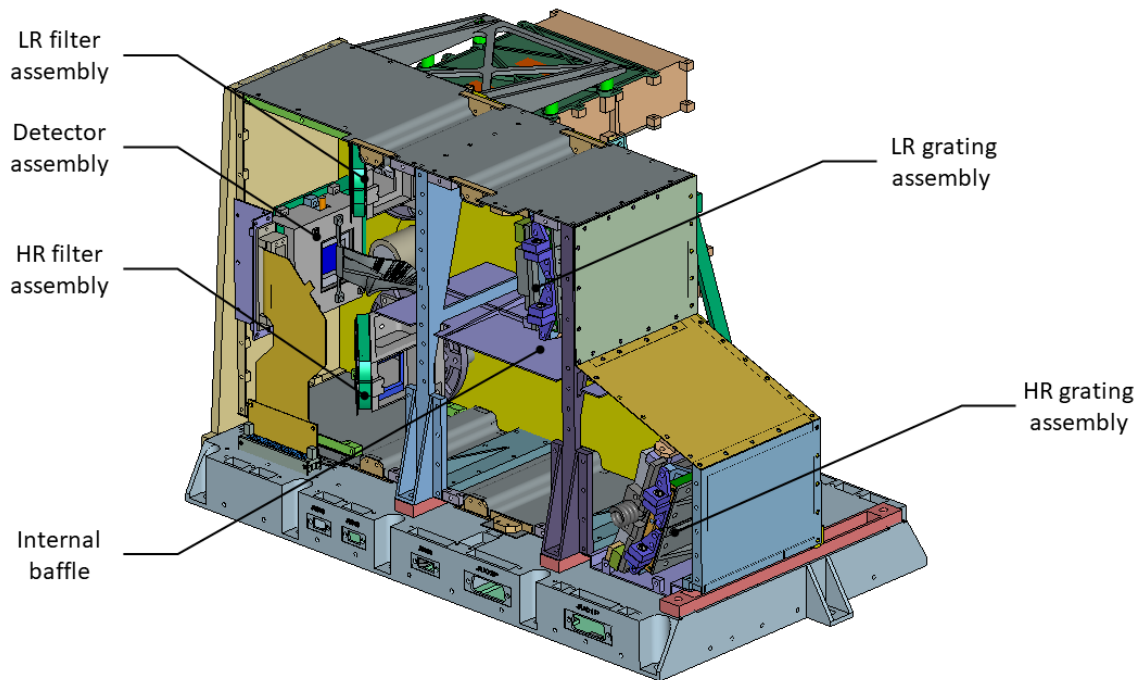


Figure 12. CAD view of the Obox

3.4 Electronics and software design

The Electronics includes three boards (figure 14), located in the Ebox:

1. The SubPSU board that receives the redounded primary power bus from the VenSpec-CCU is in charge of

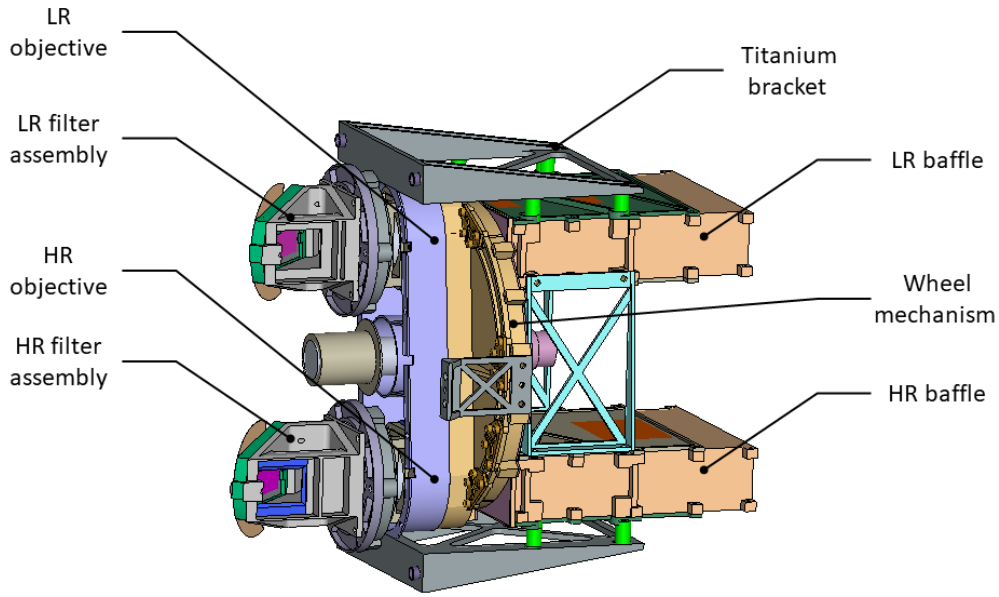


Figure 13. CAD view of the Front End optics

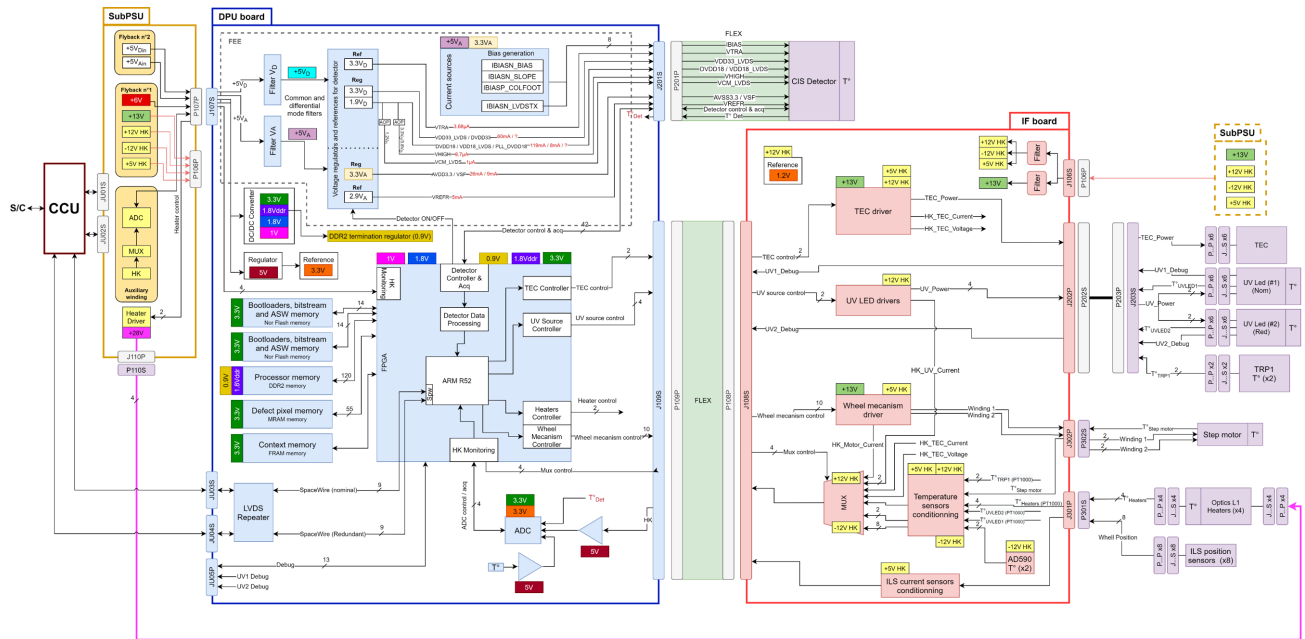


Figure 14. Electronics architecture showing the three boards, SubPSU, DPU-FEE and IF

power conversion and distribution. The SubPSU generates, from unregulated 27-33V primary power bus, the secondary voltages with galvanic isolation to supply the other electronics and instruments subsystems while the decontamination heaters are directly supplied by the primary power. The SubPSU provides also protection functions against overcurrent and overvoltage, as well as housekeeping measurements of primary current and voltages and currents of secondary output supplies;

2. The DPU-FEE board that hosts the FPGA/microprocessor and onboard software is in charge of the data interface (using redounded spacewire links for TM/TC communication with to the VenSpec-CCU), raw data processing and storage, and overall control of the instrument as well as detector interface ("Front End Electronics" - FEE). A "Debug/Test" interface is also provided with the DPU, on ground only, for extended operations with the FPGA and onboard software using a dedicated EGSE. The DPU board hosts the "FEE" section in charge of the electrical interface with the CMOS sensor (voltage/biases generation, fast readout signals interfacing, control lines,...). Special consideration is required to FEE in order to provide very stable and accurate voltages for detector polarization and current biasing by the use of linear regulators, reference voltages and common mode and differential filters;
3. The IF board ("Interface") that provides drivers and power interfaces to the subsystems, including a full bridges motor driver to control the stepper motor of the wheel mechanisms, a buck regulator for Peltier cooler, and current sources for the calibration UV sources. The IF board implements also the conditioning electronics for temperature monitoring (PT1000, AD590-transducer, and K type thermocouple), voltage and current monitoring for Peltier cooler and current monitoring of the UV LEDs.

The DPU is built around the NanoXplore NG-Ultra device that embeds a large FPGA fabric and a SoC (System-on-Chip) including multiple services and a quad core Arm-r52 processor. It hosts the onboard software, mainly in charge of subsystems control, instrument modes and sequencing, data processing and generation, TM/TC management (with PUS services), FDIR, memory management. The VenSpec-U onboard software largely relies on the implementation of LVCUGen³⁷ a Time-Space Partitioning based solution provided by CNES, using an hypervisor (Xtratum).

3.5 Contamination management

Contamination (both particulate and molecular) will be detrimental to the instrument's performances. In addition to the usual contamination control methods (clean rooms, handling, red tags like apertures covers, etc...) some specific methods and design aspects are implemented on VenSpec-U to preserve End-Of-Life (EOL) performances. First, most of the optical components are accommodated inside the Optical Cavity, which is a volume where extended restrictions apply : strict materials selection ("no glue" as a goal, no paint, limitation of number and lengths of wires and harnesses), purging during AIT/V phases, use of a zeolite trap to capture contaminants in flight, use of dust filters (frits) on venting paths, use of chicanes and labyrinths where relevant.

In case a loss of performance is still observed in flight, the front-end optics (including lenses, slits and filters) can be heated up to decontaminate the optical surfaces thanks to the decontamination heaters.

Finally, the launch phase represents a major contribution of the total accumulated contamination until EOL (VenSpec's apertures point upwards under the fairing, which is an undesirable position). A one-shot door mechanism (not yet designed) will be installed to protect the baffles apertures during launch.

3.6 Key subsystems overview

3.6.1 Detector

Sharing a unique detector between two optical channels requires flexibility. This is provided by the use of a CMOS image sensor, enabling specific readouts and timing modes. Custom developments were excluded to limit the risk in development and the Capella CIS120 (Table 6) sensor from Teledyne³⁸ was baselined at the end of phase A. This sensor is a 2048 by 2048 active pixel sensor array with a 10 μm pixel pitch and it will be used in its "Low Noise" (LN) variant (providing a 45 ke^- FWC and 7 e^- rms readout noise in rolling shutter mode), Backside Illuminated (BSI) and UV optimized with a specific coating. In order to keep the dark current low, the "TEC package" including a Peltier cooler has been selected (Fig.15). The detector assembly is made by soldering the detector electrical pins on 6-layer flex PCB harness which is connected to the DPU-FEE board on Ebox side and then routed and folded inside Obox (Fig.15).

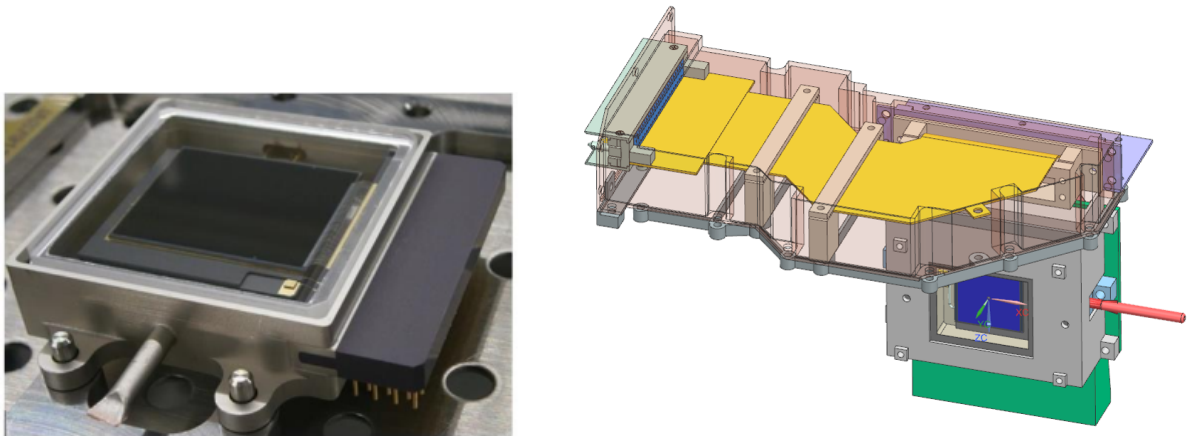


Figure 15. *Left:* TEC package of the Capella CIS120 sensor - Picture from Teledyne [38]; *Right:* CAD view of the Flex connection between the CIS120 and the DPU-FEE board

3.6.2 Wheel mechanism

The wheel mechanism is installed in front of the two apertures of the instrument and includes twelve slots. At any time, two diametrically opposed slots are therefore positioned in front of the LR and HR channels apertures (Fig.16).

The actuation of the wheel is ensured in direct drive to the wheel axis by a stepper motor (Phytron VSS19) coupled to a gearhead (ratio 1 : 196), both provided by Phytron (Fig.17). One motor step corresponds to 0.01°.

Table 6. CIS120 Generic specification overview

Parameter	Capella ^{LN}	Capella ^{LS}
Number of pixels	2048 × 2048	
Pixel size (μm^2)	10 × 10	
Image area (mm^2)	20.48 × 20.48	
Bit depth	8, 10, 12 & 14	
Operating mode	Rolling shutter (RS) Global Shutter (GS)	
Frame rate	15 fps @ 12 bit, 5 fps @ 14 bit	
QE @ 550 nm	90 %	
Q_{sat} (e^-)	45000	78000
Q_{lin} (e^-)	37000	70000
Readout noise (e^- rms)	7 in RS	12 in RS
Dark signal @ 20°C ($e^- \text{ px}^{-1} \text{ s}^{-1}$)	50 in RS, 300 in GS	
Power consumption (mW)	< 400	

The design of the mechanism includes covers, vents and chicanes to prevent the fluid lubricant used in the actuator to migrate and contaminate the optics.

Eight reed switches, each having an angular detection range of approximately 6° are in charge of the position sensing (Tab.7 in appendix, Fig.16): six of them (RS0 to RS5) are used in combination to define a unique binary code for each stable position while the two others (RS6 and RS7) are used to achieve the required fine positioning of the pinholes (precision better than 0.1°). This is done by detecting the rising edges of the reed switches while rotating the wheel.

The wheel mechanism will be mainly operated in "step mode" with a trapezoidal acceleration profile and the position will be checked once the motion is done. The POS_CC position will be reached in closed loop: the wheel will be rotated until the corresponding code (13d) is detected, a final motion of 3° will be done to center the wheel on the requested position. The POS_PP position will be reached by first detecting the corresponding code (56d) then by rotating slowly until a rising edge is detected on RS6 or RS7.

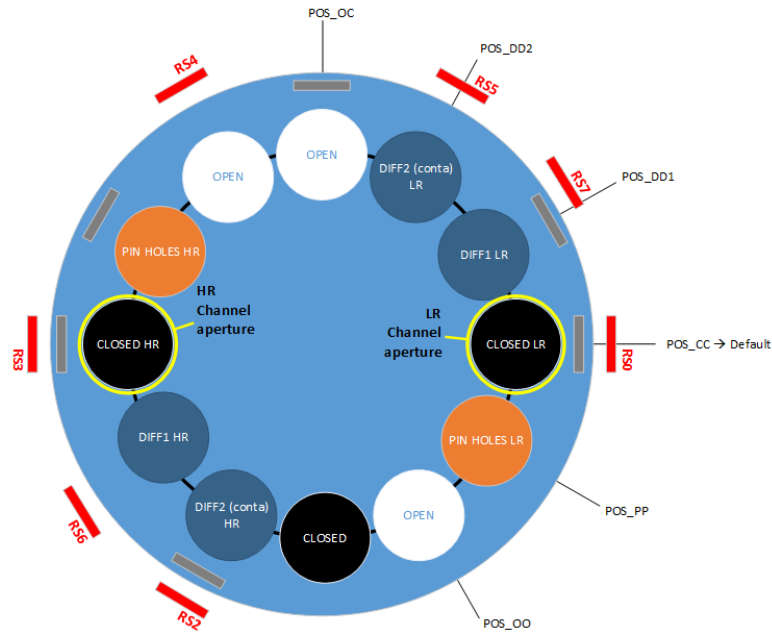


Figure 16. Wheel mechanism scheme showing the twelve slots, the position of the eight reed switches (in red) and associated magnets (in gray)

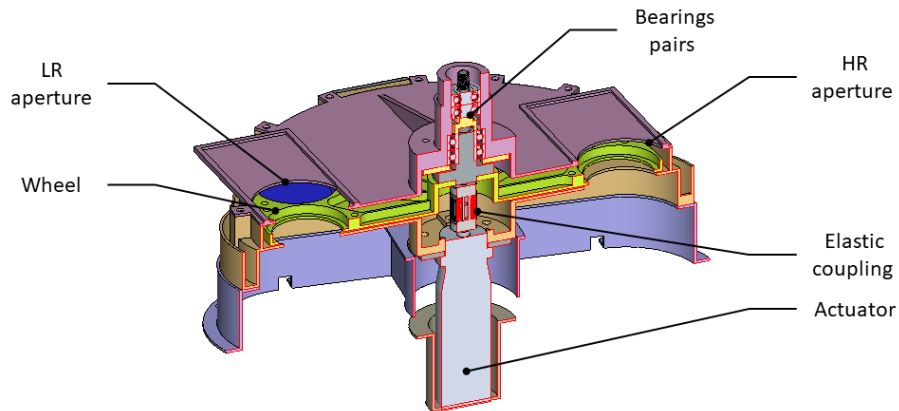


Figure 17. CAD view in cross section of the wheel mechanism

3.6.3 UV sources

VenSpec-U will use two small UV sources (one for each channel) to provide direct and homogeneous UV illumination of the CMOS sensor. It will allow doing function test during ground activities and in-flight commissioning and checkouts as well as in-flight characterizations and parameters tracking of the CMOS sensor. The main requirements for the source are to provide an adjustable and homogeneous irradiance in the spectral range of the instrument thus allowing for PRNU tracking and PTC (photon transfer curve) characterizations. Each UV source will be built around redounded surface-mount UV LEDs from OSRAM (CULBN2, 275 nm center wave-

length, 120 deg radiation, 6.3 mW radiant flux), a temperature sensor (PT1000). A pinhole coupled with a diffuser will be used to limit the irradiance on the focal plane. At the time of writing this paper, a qualification plan of the LEDs is being defined.

4. INSTRUMENT PERFORMANCES ASSESSMENT

4.1 Spectral and spatial resolutions

Spectral and spatial resolutions are estimated using the Zemax software and provisions are taken to deal with perturbations (essentially static misalignment and thermo-elastic deformations - TED).

Compliance to the 0.3 nm (HR) and 2 nm (LR) is achieved for 90% of the positions (wavelength \times field position) as shown on Figure 18.

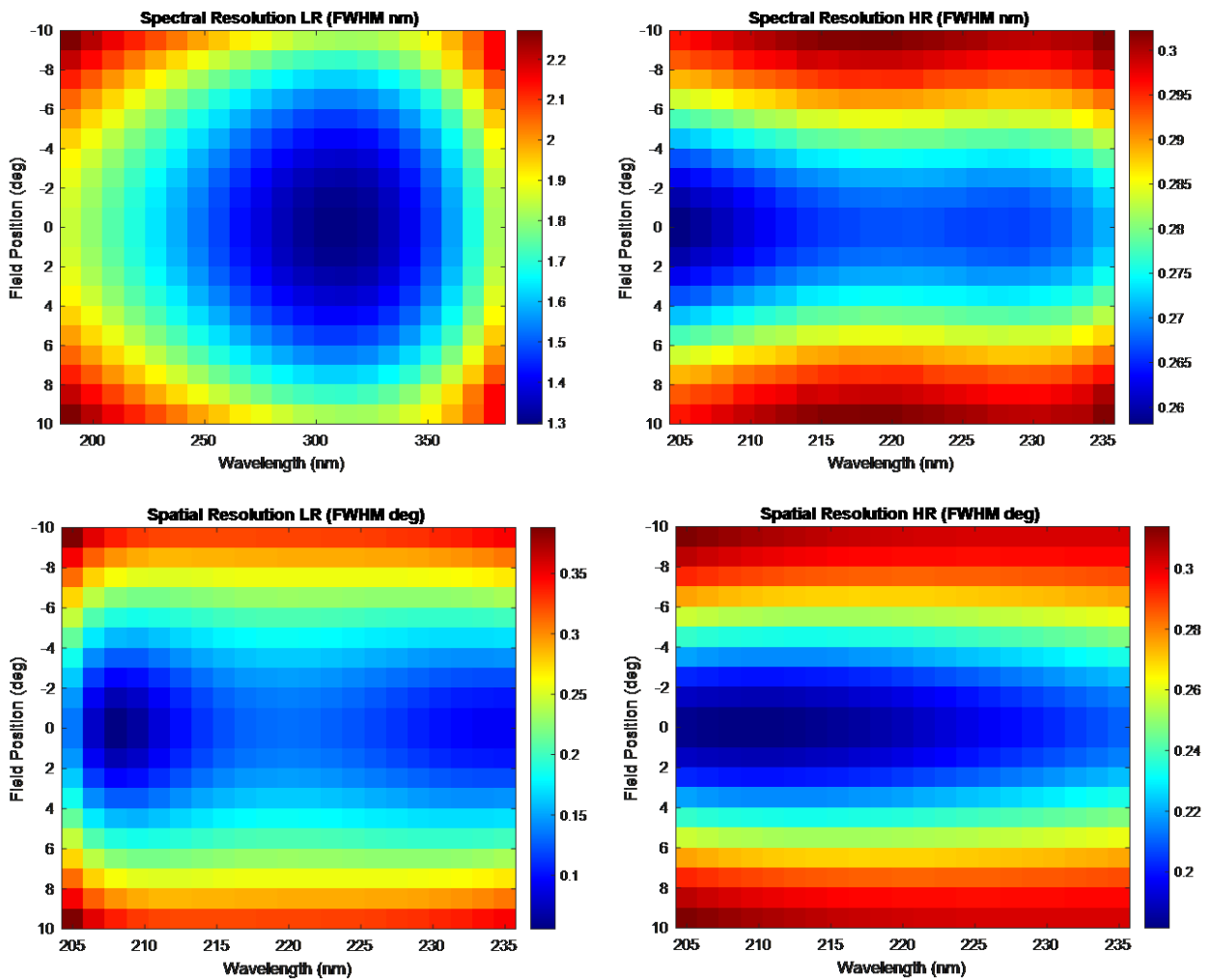


Figure 18. *Top*: Spectral resolutions achieved with the current design; *Bottom*: Spatial resolutions achieved with the current design

The current design over-performs in terms of spatial resolution (figure 18), because the spectral resolution drives the optical design and the related image quality.

4.2 Signal-to-Noise ratio on Venus

Compliance to the Signal-To-Noise ratio requirements is demonstrated using a dedicated radiometric model implementing relevant instrument parameters (optics efficiencies and optical design parameters, detector QE and random noises/biases, etc.) as well as observation geometry: altitude, Solar Zenith Angle (SZA). The performance assessments are done for several typical cases covering worst to best situations from beginning-of-life (BOL) until end-of-life (EOL).

The SNR requirement is usually easily achieved even at high SZA up to 70° and high altitude (figures 19 and 20).

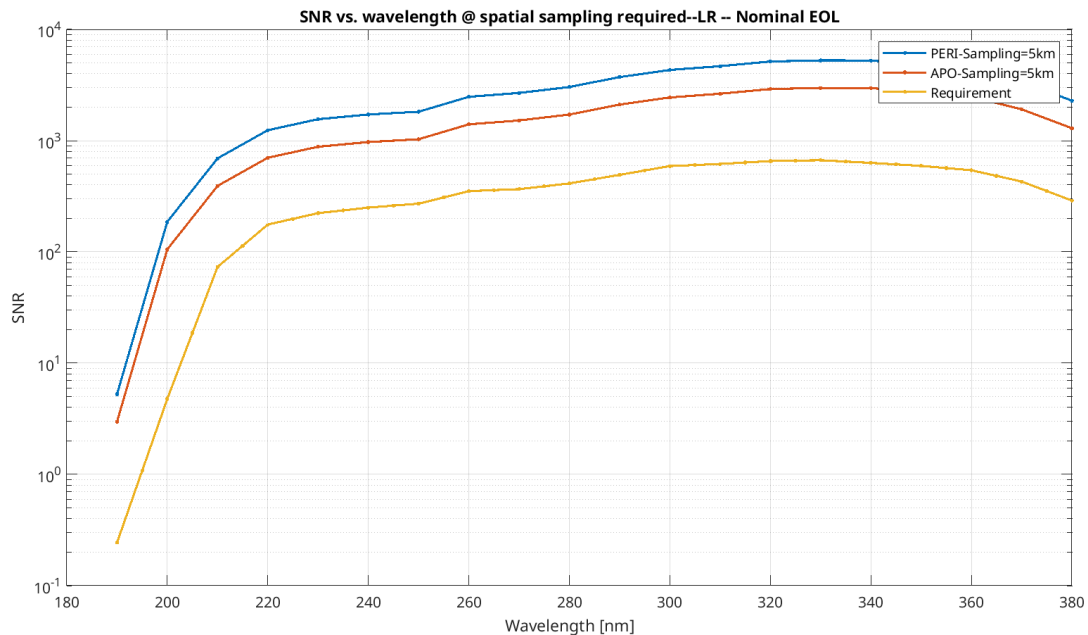


Figure 19. SNR achieved by the LR channel for a typical observation case, EOL

4.3 Effective Spectral Radiometric Accuracy and Absolute Radiometric Accuracy

A sensitivity study of the science parameters retrieval to the different measurement biases³⁵ has been performed during the last few years to investigate the impact of each type of bias related to stray-light, solar variability, polarisation, contamination, additive systematic effects, multiplicative systematic effects.

A complete "Instrument Direct Model" (IDM) is currently being built to complete the analysis and demonstrate compliance to both ESRA and ARA. This IDM will be fed up with simulated scenes (image cubes of

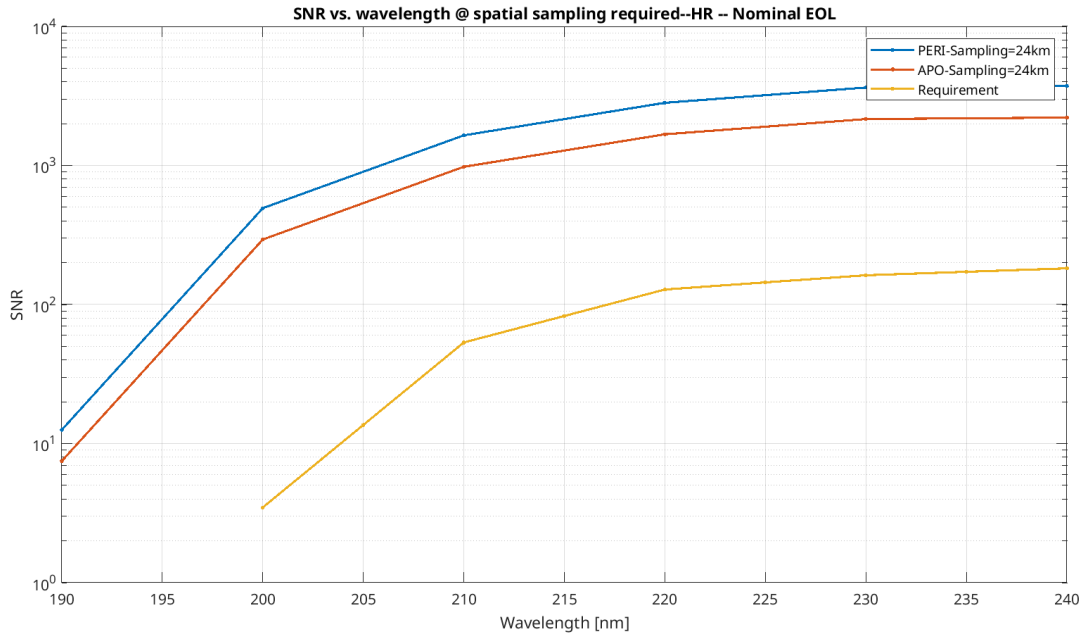


Figure 20. SNR achieved by the HR channel for a typical observation case, EOL

Venus spectral radiance) from the in-house "Radiative Transfer Model" (RTM) of Venus and will generate simulated instrument raw data taking into account best estimate instrument parameters (optical chain, detector, onboard processing). Simulated data will be then inverted (with intentionally degraded instrument parameters) using a preliminary version of the VenSpec-U pipeline (instrument and inverse RTM) to estimate atmospheric parameters thus enabling estimating the conformity of the design to ESRA and ARA requirements.

5. OPERATIONS AND OBSERVATION/INSTRUMENT MODES

The on-board software will implement four instrument modes : the standard "standby" and "safe" modes, the "science" mode, used to perform science observations as well as calibrations and the "maintenance" mode used to execute miscellaneous maintenance and diagnostic operations like low level subsystems control, decontamination, memory management, etc.

5.1 Venus observation

A typical observation of Venus (during a half-orbit, on day side, figure 21) by VenSpec-U will consist first in preparing the instrument, and then in actually performing the observation. The preparation phase will occur on night side preceding the observation and will include:

1. Instrument switch ON;

2. Instrument configuration, with subsystems parameters loading and detector cooling;
3. Acquisition of a set of reference dark frames;
4. and Opening of the wheel mechanism around the terminator crossing, while entering the day side.

The acquisition parameters (binning scheme, stacking, etc.) can be updated several times during the observation to adapt to the observing conditions and resolution requirements. Data are acquired and processed on the fly then sent to the VenSpec-CCU for compression. After the observation is complete, the instrument is reconfigured (detector is warmed up, wheel is closed) and switched OFF until the next observation opportunity.

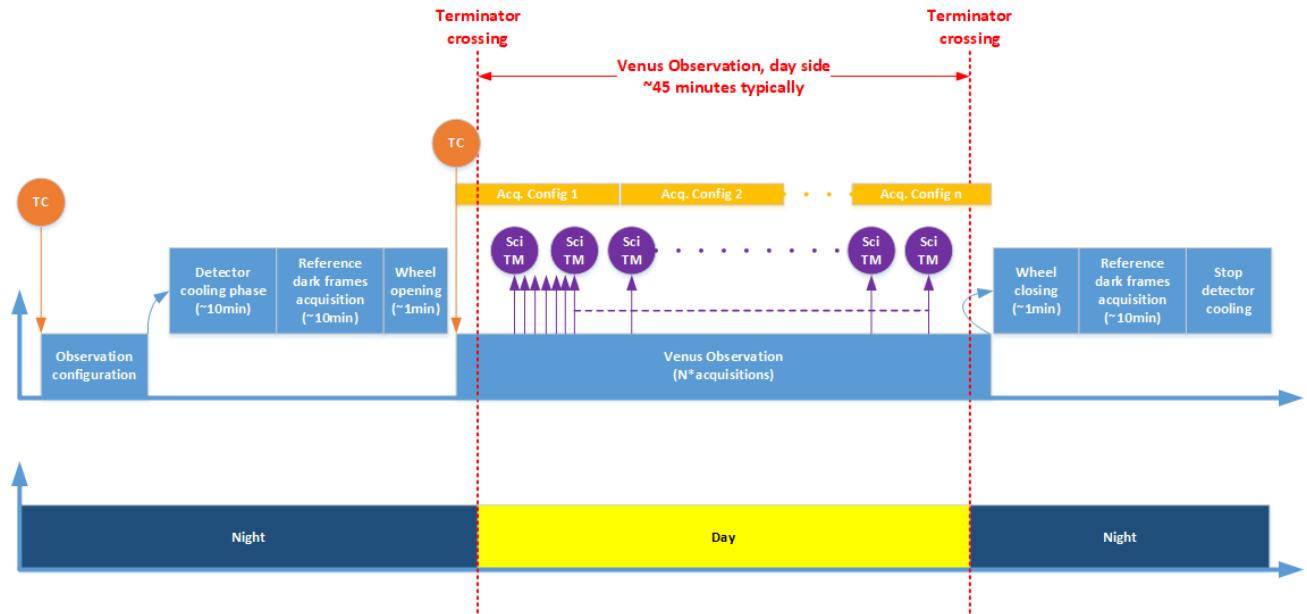


Figure 21. Operational sequence for a single orbit

The nominal operational scenario at mission level foresees that VenSpec-U will observe every day during four consecutive orbits (the so-called "VenSpec block") on day sides. Consequently, the preparation phase will occur actually only once per day, followed by four observation slots, as shown on figure 22.

5.2 Solar calibration

VenSpec-U will have some opportunities during the mission to perform radiometric calibration on the Sun. This will be achieved by off-pointing the spacecraft every 112 days such that the Sun crosses the instrument FoV.

The radiometric calibration will rely on the combination of two Sun scans. The first scan will use a set of pinholes providing the radiometric calibration for a small portion of the FoV. The pinholes are not affected by molecular contamination so the quality of this calibration method is expected to be very stable during the

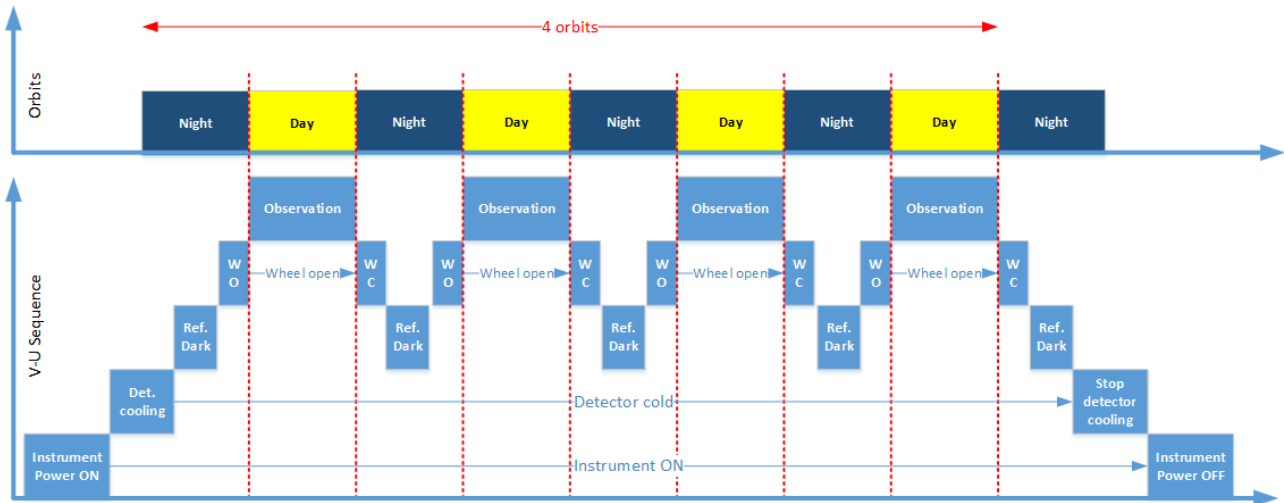


Figure 22. Operational sequence for four orbits in series ("WO" means "Wheel Open", "WC" means "Wheel Closed")

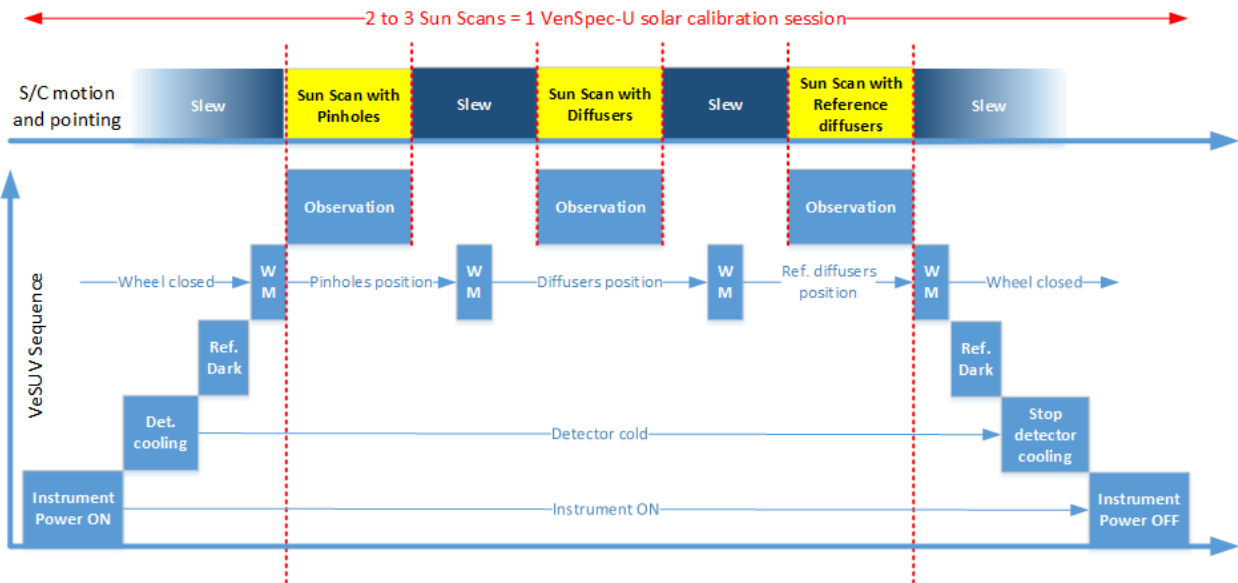


Figure 23. Operational sequence for Solar calibration ("WM" means "Wheel Motion", either to Pinholes or Diffusers position)

mission. The second scan will use a set of diffusers; these ones may be affected by molecular contamination, but will enable calibration of the full FoV.

Occasionally, a third scan will be requested to perform a calibration with another set of diffusers ("reference diffusers"). These diffusers are expected to contaminate much slowly than the nominal ones, thus enabling a relative tracking of the contamination.

5.3 Dark calibration

The calibration plan also foresees dedicated sessions to characterize and track any evolution of the dark current of the CMOS sensor. This will be done periodically for different sets of parameters such that the collected data will feed a dark current model used to support the inversion pipeline.

5.4 Internal calibration

The internal calibration, using the UV sources, will be used to perform in-flight PTC (Photon Transfer Curve), PRNU (Pixel Response Non Uniformity) characterization and diagnosis of the CMOS sensor.

6. CONCLUSION AND PERSPECTIVES

The next phase as of August 2024 (B2) will be dedicated to design maturation of the instrument and validation including some challenges (like TED management) and design verification (compliance to ESRA/ARA requirements, compliance to power and mass allocations) through multiple analyses updates (mechanical, thermal, radiations, performances, ...) as well as prototyping. In particular, a fit, form, functional and performing prototype of the optical system (named OP-B2) is being built and tested in the coming year as well as a fit, form function of the Electronics (DM-B2). Some procurement's and validation/qualifications are also either already started (gratings, detector) or shall start shortly (filters, lenses) for critical items and processes. All these activities will beneficially feed the Preliminary Design Review of the instrument scheduled for the second half of 2025.

ACKNOWLEDGMENTS

The authors wish to acknowledge the outstanding contribution of involved CNES experts to the development of the VenSpec-U instrument. BL, SB, NR, ADD, RHK, CM, SR, AV, FV, ES, WR, LB, GG, CG, AL, RM, NNT, TB, SV, JL and EM acknowledge CNES and ESA funding for all activities related to VenSpec-U and EnVision. IAA team acknowledges financial support from project PID2021-126365NB-C21 (MCI/AEI/FEDER, UE). SR thanks the Belgian Science Policy Office (BELSPO) for their support (4000144206), and the the ESA Prodex Office for the financial and contractual coordination.

REFERENCES

- [1] EnVision Science Study Team and ESA Study Team, "EnVision Definition Study Report (Red Book)," tech. rep., ESA (2024).

- [2] Helbert et. al, “The VenSpec Suite Organization: Collaborative development from instrument proposal to scientific analysis,” in [*Infrared Remote Sensing and Instrumentation XXXII*], **This volume**, SPIE (2024).
- [3] Fitzner et. al, “Electrical integration of the VenSpec spectrometer consortium: an architecture trade-off ,” in [*Infrared Remote Sensing and Instrumentation XXXII*], **This volume**, SPIE (2024).
- [4] Helbert, J., Säuberlich, T., Dyar, M. D., Ryan, C., Walter, I., Reess, J.-M., Rosas-Ortiz, Y., Peter, G., Maturilli, A., and Arnold, G., “The Venus Emissivity Mapper (VEM): advanced development status and performance evaluation,” in [*Infrared Remote Sensing and Instrumentation XXVIII*], Strojnik, M., ed., *Society of Photo-Optical Instrumentation Engineers (SPIE) Conference Series* **11502**, 1150208 (Aug. 2020).
- [5] Neefs, E., Vandaele, A. C., De Cock, R., Erwin, J., Robert, S., Thomas, I. R., Berkenbosch, S., Jacobs, L., Bogaert, P., Beeckman, B., Brassine, A., Messios, N., De Donder, E., Bolsée, D., Pereira, N., Tackley, P., Gerya, T., Kögl, S., Kögl, P., Gröbelbauer, H.-P., Wirz, F., Székely, G., Eaton, N., Roibás-Millán, E., Torralbo, I., Rubio-Arnaldo, H., Alvarez, J. M., Navajas Ortega, D., De Vos, L., Sørensen, R., Moelans, W., Algoedt, A., Blau, M., Stam, D., Renotte, E., Klinkenberg, P., Borguet, B., Thomas, S., Vervaeke, M., Thienpont, H., Castro, J. M., and Jimenez, J., “VenSpec-H spectrometer on the ESA EnVision mission: Design, modeling and analysis,” *Acta Astronautica (accepted)* (2024).
- [6] Marcq, E., Montmessin, F., Lasue, J., Bézard, B., Jessup, K. L., Lee, Y. J., Wilson, C. F., Lustrement, B., Rouanet, N., and Guignan, G., “Instrumental requirements for the study of Venus’ cloud top using the UV imaging spectrometer VeSUV,” *Advances in Space Research* **68**, 275–291 (July 2021).
- [7] Esposito, L. W., Copley, M., Eckert, R., Gates, L., Stewart, A. I. F., and Worden, H., “Sulfur dioxide at the Venus cloud tops, 1978 - 1986.,” *J. Geophys. Res.* **93**, 5267–5276 (May 1988).
- [8] Zasova, L. V., Moroz, V. I., Esposito, L. W., and Na, C. Y., “SO₂ in the Middle Atmosphere of Venus: IR Measurements from Venera-15 and Comparison to UV Data,” *Icarus* **105**, 92–109 (Sept. 1993).
- [9] Marcq, E., Belyaev, D., Montmessin, F., Fedorova, A., Bertaux, J.-L., Vandaele, A. C., and Neefs, E., “An investigation of the SO₂ content of the venusian mesosphere using SPICAV-UV in nadir mode,” *Icarus* **211**, 58–69 (Jan. 2011).
- [10] Marcq, E., Bertaux, J.-L., Montmessin, F., and Belyaev, D., “Variations of sulphur dioxide at the cloud top of Venus’s dynamic atmosphere,” *Nature Geoscience* **6**, 25–28 (Jan. 2013).
- [11] Marcq, E., Lea Jessup, K., Baggio, L., Encrenaz, T., Lee, Y. J., Montmessin, F., Belyaev, D., Korablev, O., and Bertaux, J.-L., “Climatology of SO₂ and UV absorber at Venus’ cloud top from SPICAV-UV nadir dataset,” *Icarus* **335**, 113368 (Jan. 2020).

- [12] Encrenaz, T., Greathouse, T. K., Roe, H., Richter, M., Lacy, J., Bézard, B., Fouchet, T., and Widemann, T., “HDO and SO₂ thermal mapping on Venus: evidence for strong SO₂ variability,” *A&A* **543**, A153 (July 2012).
- [13] Encrenaz, T., Greathouse, T. K., Giles, R., Widemann, T., Bézard, B., Lefèvre, M., and Shao, W., “HDO and SO₂ thermal mapping on Venus. VI. Anomalous SO₂ behavior during late 2021,” *A&A* **674**, A199 (June 2023).
- [14] Marcq, E., Mills, F. P., Parkinson, C. D., and Vandaele, A. C., “Composition and Chemistry of the Neutral Atmosphere of Venus,” *Space Sci. Rev.* **214**, 10 (Feb. 2018).
- [15] Tellmann, S., Häusler, B., Hinson, D. P., Tyler, G. L., Andert, T. P., Bird, M. K., Imamura, T., Pätzold, M., and Remus, S., “Small-scale temperature fluctuations seen by the VeRa Radio Science Experiment on Venus Express,” *Icarus* **221**, 471–480 (Nov. 2012).
- [16] Lefèvre, M., Lebonnois, S., and Spiga, A., “Three-Dimensional Turbulence-Resolving Modeling of the Venusian Cloud Layer and Induced Gravity Waves: Inclusion of Complete Radiative Transfer and Wind Shear,” *Journal of Geophysical Research (Planets)* **123**, 2773–2789 (Oct. 2018).
- [17] Mori, R., Imamura, T., Ando, H., Häusler, B., Pätzold, M., and Tellmann, S., “Gravity Wave Packets in the Venusian Atmosphere Observed by Radio Occultation Experiments: Comparison With Saturation Theory,” *Journal of Geophysical Research (Planets)* **126**, e06912 (Sept. 2021).
- [18] Esposito, L. W., “Sulfur Dioxide: Episodic Injection Shows Evidence for Active Venus Volcanism,” *Science* **223**, 1072–1074 (Mar. 1984).
- [19] Mills, F. P. and Allen, M., “A review of selected issues concerning the chemistry in Venus’ middle atmosphere,” *Planet. Space Sci.* **55**, 1729–1740 (Oct. 2007).
- [20] Jessup, K. L., Marcq, E., Mills, F., Mahieux, A., Limaye, S., Wilson, C., Allen, M., Bertaux, J.-L., Markiewicz, W., Roman, T., Vandaele, A.-C., Wilquet, V., and Yung, Y., “Coordinated Hubble Space Telescope and Venus Express Observations of Venus’ upper cloud deck,” *Icarus* **258**, 309–336 (Sept. 2015).
- [21] Ross, F. E., “No. 363. Photographs of Venus.,” *Contributions from the Mount Wilson Observatory / Carnegie Institution of Washington* **363**, 1–36 (Jan. 1928).
- [22] Frandsen, B. N., Wennberg, P. O., and Kjaergaard, H. G., “Identification of OSSO as a near-UV absorber in the Venusian atmosphere,” *Geophys. Res. Lett.* **43**, 11,146–11,155 (Nov. 2016).
- [23] Krasnopolsky, V. A., “On the iron chloride aerosol in the clouds of Venus,” *Icarus* **286**, 134–137 (Apr. 2017).

- [24] Horinouchi, T., Kouyama, T., Lee, Y. J., Murakami, S.-y., Ogohara, K., Takagi, M., Imamura, T., Nakajima, K., Peralta, J., Yamazaki, A., Yamada, M., and Watanabe, S., “Mean winds at the cloud top of Venus obtained from two-wavelength UV imaging by Akatsuki,” *Earth, Planets and Space* **70**, 10 (Jan. 2018).
- [25] Patsaeva, M. V., Khatuntsev, I. V., Zasova, L. V., Hauchecorne, A., Titov, D. V., and Bertaux, J. L., “Solar-Related Variations of the Cloud Top Circulation Above Aphrodite Terra From VMC/Venus Express Wind Fields,” *Journal of Geophysical Research (Planets)* **124**, 1864–1879 (July 2019).
- [26] Markiewicz, W. J., Titov, D. V., Ignatiev, N., Keller, H. U., Crisp, D., Limaye, S. S., Jaumann, R., Moissl, R., Thomas, N., Esposito, L., Watanabe, S., Fiethe, B., Behnke, T., Szemerey, I., Michalik, H., Perplies, H., Wedemeier, M., Sebastian, I., Boogaerts, W., Hviid, S. F., Dierker, C., Osterloh, B., Böker, W., Koch, M., Michaelis, H., Belyaev, D., Dannenberg, A., Tschimmel, M., Russo, P., Roatsch, T., and Matz, K. D., “Venus Monitoring Camera for Venus Express,” *Planet. Space Sci.* **55**, 1701–1711 (Oct. 2007).
- [27] Yamazaki, A., Yamada, M., Lee, Y. J., Watanabe, S., Horinouchi, T., Murakami, S.-y., Kouyama, T., Ogohara, K., Imamura, T., Sato, T. M., Yamamoto, Y., Fukuhara, T., Ando, H., Sugiyama, K.-i., Takagi, S., Kashimura, H., Ohtsuki, S., Hirata, N., Hashimoto, G. L., Suzuki, M., Hirose, C., Ueno, M., Satoh, T., Abe, T., Ishii, N., and Nakamura, M., “Ultraviolet imager on Venus orbiter Akatsuki and its initial results,” *Earth, Planets and Space* **70**, 23 (Feb. 2018).
- [28] Lee, Y. J., Imamura, T., Schröder, S. E., and Marcq, E., “Long-term variations of the UV contrast on Venus observed by the Venus Monitoring Camera on board Venus Express,” *Icarus* **253**, 1–15 (June 2015).
- [29] Lee, Y. J., Kopparla, P., Peralta, J., Schröder, S. E., Imamura, T., Kouyama, T., and Watanabe, S., “Spatial and Temporal Variability of the 365-nm Albedo of Venus Observed by the Camera on Board Venus Express,” *Journal of Geophysical Research (Planets)* **125**, e06271 (June 2020).
- [30] Khatuntsev, I. V., Patsaeva, M. V., Titov, D. V., Zasova, L. V., Ignatiev, N. I., and Gorinov, D. A., “Twelve-Year Cycle in the Cloud Top Winds Derived from VMC/Venus Express and UVI/Akatsuki Imaging,” *Atmosphere* **13**, 2023 (Dec. 2022).
- [31] Markiewicz, W. J., Titov, D. V., Limaye, S. S., Keller, H. U., Ignatiev, N., Jaumann, R., Thomas, N., Michalik, H., Moissl, R., and Russo, P., “Morphology and dynamics of the upper cloud layer of Venus,” *Nature* **450**, 633–636 (Nov. 2007).
- [32] Piccialli, A., Titov, D. V., Sanchez-Lavega, A., Peralta, J., Shalygina, O., Markiewicz, W. J., and Svedhem, H., “High latitude gravity waves at the Venus cloud tops as observed by the Venus Monitoring Camera on board Venus Express,” *Icarus* **227**, 94–111 (Jan. 2014).
- [33] Fukuhara, T., Futaguchi, M., Hashimoto, G. L., Horinouchi, T., Imamura, T., Iwagaimi, N., Kouyama, T., Murakami, S.-Y., Nakamura, M., Ogohara, K., Sato, M., Sato, T. M., Suzuki, M., Taguchi, M., Takagi, S.,

- Ueno, M., Watanabe, S., Yamada, M., and Yamazaki, A., “Large stationary gravity wave in the atmosphere of Venus,” *Nature Geoscience* **10**, 85–88 (Jan. 2017).
- [34] Lefèvre, M., Marcq, E., and Lefèvre, F., “The impact of turbulent vertical mixing in the Venus clouds on chemical tracers,” *Icarus* **386**, 115148 (Nov. 2022).
- [35] Conan, Lucile and Marcq, Emmanuel and Lustrement, Benjamin and Rouanet, Nicolas and Parc, Léna and Bertran, Sandrine and Helbert, Jörn and Vandaele, Ann Carine and Alemanno, Giulia, “The VenSpec-U Spectrometer onboard EnVision mission: a Sensitivity Study,” **This volume**, SPIE (2024).
- [36] Chassefière, E., Maria, J.-L., Goutail, J.-P., and Leblanc, F. e. a., “PHEBUS: A double ultraviolet spectrometer to observe Mercury’s exosphere,” *Planetary and Space Science* **58**(1), 201–223 (2010).
- [37] Galizzi, J., Metge, J.-J., Arberet, P., Morand, E., Vigeant, F., Crespo, A., Masmano, M., Coronel Parada, J., Ripoll, I., and Brocal, V., “LVCUGEN (TSP-based solution) and first porting feedback,” **erts2012**, **hal-02192398**, HAL (2012).
- [38] Otero, R. G., Mackie, R., Greenaway, C., Lemon, T., Jerram, P., and Pratlong, J., “Capella: CIS120 general purpose CMOS sensor for space applications,” in [*International Conference on Space Optics — ICSSO 2020*], Cugny, B., Sodnik, Z., and Karafolas, N., eds., **11852**, 118520S, International Society for Optics and Photonics, SPIE (2021).

APPENDIX A. TABLES

Position	Angular position from POS_CC (deg)	Binary code (LSB is RS0)	Decimal code
POS_CC	0	001101	13
POS_DD1	30 CW	110001	49
POS_DD2	60 CW	011010	26
POS_OC	90 CW	100011	35
POS_OO-180	Nominally not used	110100	52
POS_PP-180	Nominally not used	000111	7
POS_CC-180	Nominally not used	101001	41
POS_DD1-180	Nominally not used	001110	14
POS_DD2-180	Nominally not used	010011	19
POS_CO	90 CCW	011100	28
POS_OO	60 CCW	100110	38
POS_PP	30 CCW	111000	56

Table 7. Position encoding provided by the reed switches